# Emergence of Domains and Nonlinear Transport in the Zero-Resistance State

I. A. Dmitriev,[1,2,3,4] M. Khodas,[5] A. D. Mirlin,[2,3,6] and D. G. Polyakov[3]
[1]*Max Planck Institute for Solid State Research, 70569 Stuttgart, Germany*
[2]*Institut für Theorie der Kondensierten Materie and DFG Center for Functional Nanostructures, Karlsruhe Institute of Technology, 76128 Karlsruhe, Germany*
[3]*Institut für Nanotechnologie, Karlsruhe Institute of Technology, 76021 Karlsruhe, Germany*
[4]*Ioffe Physical Technical Institute, 194021 St. Petersburg, Russia*
[5]*Department of Physics and Astronomy, University of Iowa, Iowa City, Iowa 52242, USA*
[6]*Petersburg Nuclear Physics Institute, 188300 St. Petersburg, Russia*
(Received 5 May 2013; published 11 November 2013)

We study transport in the domain state, the so-called zero-resistance state, that emerges in a two-dimensional electron system in which the combined action of microwave radiation and magnetic field produces a negative absolute conductivity. We show that the voltage-biased system has a rich phase diagram in the system size and voltage plane, with second- and first-order transitions between the domain and homogeneous states for small and large voltages, respectively. We find the residual negative dissipative resistance in the stable domain state.

DOI: 10.1103/PhysRevLett.111.206801 PACS numbers: 73.50.−h, 64.60.−i

*Introduction.*—The zero-resistance state (ZRS) [1–4] is perhaps the most spectacular of the newly discovered nonequilibrium effects in ultrahigh mobility two-dimensional (2D) electron systems in high Landau levels [5]. The ZRS is attributed [6] to the instability of a homogeneous state with the negative *absolute* dissipative conductivity $\sigma < 0$ and the associated nonequilibrium phase transition into a *static* domain state with zero net resistance [7–12]. The domain picture is supported by a number of experiments [13–20]. Similar electrical instabilities have also been known to appear in other contexts [5,21,22], most prominently, in the Gunn diode [23] (where, however, most of the effects are due to the emergence of moving domains) and in illuminated ruby crystals [24–26] (where the strongly anisotropic nature of charge transport reduces the problem to one dimension). Whereas the microscopic mechanisms that lead to $\sigma < 0$ in nonequilibrium 2D electron gases in the presence of a magnetic field $B$ are by now fairly well established [5], the physics of the resulting domain state remains poorly understood.

Most works [6–12] so far have studied the bulk properties of the domain state, i.e., the limit $d/L \to 0$ in which the width $d$ of the domain wall (DW) is vanishingly small compared to the system size $L$. In fact, however, the physics related to the DW structure is crucially important near the phase transition, because the DW width diverges at the critical point.

In this Letter, we develop an analytical model of the domain state for arbitrary $d/L$ and study the nonlinear response of the domain state to external voltage. The analytical solution enables us to construct the phase diagram of the biased finite-size system, which incorporates continuous and discontinuous transitions between the homogeneous and domain states, and to calculate the negative conductance in the domain state.

*Model.*—Consider 2D electrons occupying a stripe ($|x| < L/2$, $z = 0$), infinite in the $y$ direction [Fig. 1(a)], between two plane metallic contacts at $x = \pm L/2$ that are perpendicular to the stripe. Under the illumination by microwaves at $B \neq 0$, the linear response dc dissipative conductivity $\sigma(E \to 0)$, where $E$ is the dc driving field, becomes negative in one or more intervals of $B$ for the microwave power $P$ above the threshold $P_c$ [5]. The nonlinear absolute conductivity $\sigma(E)$ remains negative in a finite range of $E$, crossing zero at the critical field $E_c$ [Fig. 1(b)] [27]. By contrast, the diffusion coefficient $D > 0$ is nearly unaffected by the radiation.

We first explore the part of the phase diagram in which the system at $P \neq 0$ remains homogeneous along the stripe so that the surface electron density $n_e(x)$ and the $x$ and $y$ components of the electric current $j_{x,y}(x)$ depend on $x$ only. The domain state is a stable solution of the Poisson and continuity equations. The former relates $n_e(x)$ to the

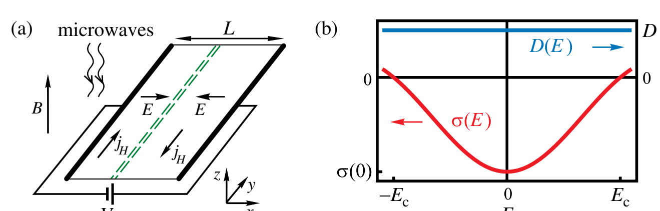


FIG. 1 (color online). (a) Geometry of the model: a 2D stripe between two metallic contacts along the long sides. The domain wall (double dashed line) and the electric field $E$ and the Hall current $j_H$ are shown for the voltage-biased domain state. (b) The nonlinear dissipative conductivity $\sigma(E)$ and the diffusion coefficient $D = \text{const}(E)$.

 

normal component $\mathcal{E}_z(x,z)$ of the electric field: $2\pi e[n_e(x)-n_0]=\epsilon\mathcal{E}_z(x,+0)$ with $e<0$, where $n_0$ is the density of background positive charges and $\epsilon$ is the dielectric constant of the medium. The continuity equation reduces to $\partial_x j_x(x)=0$. We assume that the in-plane electric field $E(x)=\mathcal{E}_x(x,+0)$ varies on a spatial scale that is larger than the microscopic scales [28] and introduce the local conductivity $\sigma[E(x)]$. Note that the Einstein relation does not hold at $P\neq 0$ and the current $j_x=\sigma(E)E-eD\partial_x n_e$ is not expressible as the gradient of the electrochemical potential [29].

At $z\neq 0$, the functions $\mathcal{E}_x(x,z)$ and $\mathcal{E}_z(x,z)$ are harmonic conjugates. This, together with the continuity of $\mathcal{E}_x(x,z)$ at $z=0$, allows us to represent the Poisson equation as $\epsilon E(x)=2\pi e\mathcal{H}\{n_e(x)\}$, where the Hilbert transform $\mathcal{H}\{f(x)\}\equiv\pi^{-1}\mathrm{p.v.}\int dx'(x-x')^{-1}f(x')$ obeys $\mathcal{H}^2=-1$ (where "p.v." = principal value). Applying the Hilbert transform to the Poisson equation in this form and substituting the result in the diffusion term in $j_x$, we find that $E(x)$ satisfies $E(x)\sigma[E(x)]+(\epsilon D/2\pi)\partial_x\mathcal{H}\{E(x)\}=j_x$. Below, we solve this equation with the boundary conditions $n_e(x=\pm L/2)=n_0$ for the case of

$$\sigma(E)=\sigma(0)(E_c/\pi E)\sin(\pi E/E_c) \tag{1}$$

with $\sigma(0)<0$ [Fig. 1(b)] [30]. By introducing the dimensionless field $\theta(x)=\pi E(x)/2E_c$, density $\rho(x)=\pi^2 e[n_e(x)-n_0]/\epsilon E_c$, and current $\tilde{j}=\pi j_x/\sigma(0)E_c$, we thus have

$$\sin 2\theta+2\lambda\partial_x\rho=\tilde{j}, \tag{2}$$

where $\rho(x)$ and $\theta(x)$ satisfy $\rho(x)=-\mathcal{H}\{\theta(x)\}$ and

$$\lambda=\epsilon D/2\pi|\sigma(0)|. \tag{3}$$

Being the only spatial scale in Eq. (2) at $\tilde{j}=0$, $\lambda$ is identified as the nonequilibrium screening length.

*Domain solution.*—With the boundary conditions $\rho(\pm L/2)=0$, the domain solution to Eq. (2) in terms of the complex function $\Psi_{\mathrm{dom}}=\theta_{\mathrm{dom}}+i\rho_{\mathrm{dom}}$ reads

$$\Psi_{\mathrm{dom}}=i\ln\frac{\cosh(\xi-iw)}{\sinh\xi}-\frac{\arcsin\tilde{j}}{2}, \tag{4}$$

where $2\xi=i\pi x/L+iw+\beta$, $w=\arctan(\tilde{j}l)$, $\beta=\mathrm{arcoth}\sqrt{l^2-\tilde{j}^2l^2}$, and $l=L/\pi\lambda$. The system spontaneously chooses between two degenerate states related by $\Psi_{\mathrm{dom}}(x)\leftrightarrow\Psi^*_{\mathrm{dom}}(-x)$; for definiteness, we analyze the solution with $\theta_{\mathrm{dom}}(L/2)>0$.

*Homogeneous state: linear stability.*—In the homogeneous case of $\rho=0$, Eq. (2) gives $\theta^<_{\mathrm{hom}}=(1/2)\arcsin\tilde{j}$ and $\theta^>_{\mathrm{hom}}=\pi/2-\theta^<_{\mathrm{hom}}$, where the signs $\lessgtr$ correspond to the negative (<) and positive (>) differential conductivity $\sigma_d(E)=\partial_E[E\sigma(E)]=\sigma(0)\cos 2\theta$. Linear stability analysis [31] around this solution shows that it is stable against small charge fluctuations proportional to $\exp(iq_x x+iq_y y)$ if

$$\sigma_d(E)q_x^2+\sigma(E)q_y^2>-(\epsilon D/2\pi)(q_x^2+q_y^2)^{3/2} \tag{5}$$

for all possible $q_x$ and $q_y$. In an infinite 2D system, Eq. (5) reduces to the usual stability conditions $\sigma_d>0$ for longitudinal and $\sigma>0$ for transverse fluctuations. In the stripe geometry, $q_x$ takes discrete values and the diffusion term in Eq. (5) becomes relevant, with

$$\sigma_d(E)>-\epsilon D/2L \tag{6}$$

as the condition of the longitudinal stability ($q_y=0$, $|q_x|=\pi/L$). For $E\to 0$, Eq. (6) gives the threshold value of $l=1$ [32] for the breakup of the homogeneous state into domains in the unbiased case, as discussed below.

*Unbiased domain state.*—For $\tilde{j}=0$, Eq. (4) reduces to

$$\theta_{\mathrm{dom}}=\arctan[(l^2-1)^{1/2}\sin(\pi x/L)], \tag{7}$$

$$\rho_{\mathrm{dom}}=\mathrm{artanh}[(1-l^{-2})^{1/2}\cos(\pi x/L)] \tag{8}$$

[Figs. 2(a) and 2(b)]. In the limit $l\gg 1$, Eq. (7) simplifies to $\theta_{\mathrm{dom}}=\arctan(x/\lambda)$, which means two domains with $E(\pm L/2)\simeq\pm E_c$ separated by the DW of width $\lambda$. The DW is charged with $\rho(x)\simeq\ln(L/|x|)$ for $\lambda\ll|x|\ll L$. This gives the oppositely directed Hall currents $j_y(x)=-en_e(x)cE(x)/B$ on the sides of the DW [Fig. 1(a)]. With the lowering of $l$, both $|\theta(x)|$ and $\rho(x)$ decrease and vanish at $l=1$. The homogeneous state with $\sigma(0)<0$ is stable for $l<1$ [Eq. (6)]; i.e., there is a continuous transition between the homogeneous and domain states. For $0<l-1\ll 1$, $\Psi_{\mathrm{dom}}\simeq i\sqrt{2(l-1)}\exp(-i\pi x/L)$ vanishes with the critical exponent 1/2.

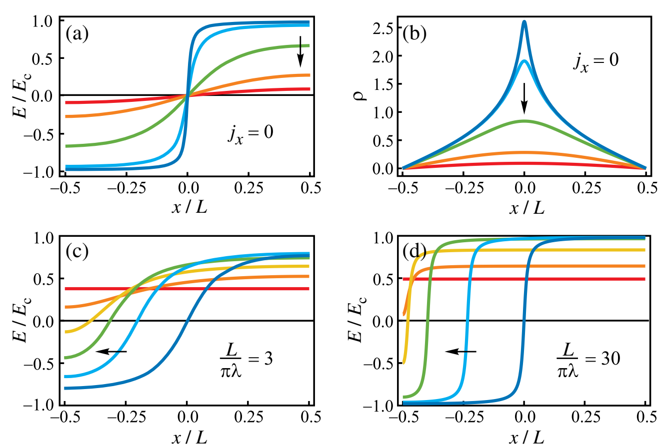


FIG. 2 (color online). Spatial distribution of (a) the electric field $E(x)$ (in units of $E_c$) and (b) the charge density (in units of $\pi^2 e/\epsilon E_c$) $\rho(x)$ in the domain state of the unbiased stripe (current $j_x=0$) for $L/\pi\lambda=30$, 10, 2, 1.1, 1.01 ($L$ decreases in the direction of arrow). As the current is increased, the domain wall is shifted and broadened. The field $E(x)$ is shown for (c) $L/\pi\lambda=3$ and the current [in units of $\sigma(0)E_c/\pi$] $\tilde{j}=0$, 0.25, 0.5, 0.75, 0. 9, $(8/9)^{1/2}$ and for (d) $L/\pi\lambda=30$ and $\tilde{j}=0$, 0.03, 0.1, 0.5, 0.9, $(899/900)^{1/2}$ ($\tilde{j}$ grows in the direction of arrow).

*Biased domain state.*—For $\tilde{j} \neq 0$, Eq. (4) tells us that the DW shifts by $Lw/\pi$ from $x = 0$ while the characteristic width of the DW $d = L\beta/\pi$ grows with increasing $|\tilde{j}|$ [Figs. 2(c) and 2(d)] and diverges as $(\tilde{j}_{c2} - |\tilde{j}|)^{-1/2}$ at the critical point $|\tilde{j}| = \tilde{j}_{c2} \equiv (1 - l^{-2})^{1/2}$. According to Eq. (6), for $|\tilde{j}| > \tilde{j}_{c2}$ the homogeneous state $\theta_{\text{hom}}$ is longitudinally stable. The line $\tilde{j}_{c2}(l)$ of the second-order transitions includes, at its end point $l = 1$, the transition in the unbiased stripe discussed above.

Averaging the field $\theta_{\text{dom}}$ [Eq. (4)] over the stripe cross section, $\bar{\theta}_{\text{dom}} = (1/L)\int_{-L/2}^{L/2} dx\theta_{\text{dom}}(x)$, one finds the bias voltage $V = 2E_c L\bar{\theta}_{\text{dom}}/\pi$, i.e., the current-voltage characteristic (CVC) of the domain state

$$\bar{\theta}_{\text{dom}} = \arctan(\tilde{j}l) - (1/2)\arcsin\tilde{j}. \qquad (9)$$

Note that the current $j_x$ flows against the applied field $j_x V < 0$. For $V \to 0$, Eq. (9) gives $\bar{\theta}_{\text{dom}} = (l - 1/2)\tilde{j}$ or, restoring units, the linear dissipative conductance of the stripe $j_x/V = \langle\sigma\rangle/L$ in the domain state, where

$$\langle\sigma\rangle = \sigma(0)(2L/\pi\lambda - 1)^{-1}, \qquad L > \pi\lambda \qquad (10)$$

(see inset in Fig. 3). It is worth noting that, as $L$ increases, $\langle\sigma\rangle$ in Eq. (10) behaves as $L^{-1}$ in sharp contrast to the exponential behavior of $\langle\sigma\rangle \propto -\exp(-L/\lambda_{3D})$ [8,26] for a three-dimensional (3D) medium with the negative conductivity ($\lambda_{3D}$ is the analogue of $\lambda$), where the relation between the electric field and charge density is local. Transport across the DW is thus strongly enhanced by the nonlocal character of 2D electrostatics. The CVC (9) for several values of $l$ is shown by the dashed lines in Fig. 4. For $l > \sqrt{2}$, the current is seen to become, as the voltage is increased, a double-valued function of $V$. That is, in fact, the continuous transition line in the $V$-$l$ plane terminates at $l = \sqrt{2}$ and becomes first order for larger $l$ (Fig. 3), as we discuss next.

*Lyapunov functional.*—The linear stability analysis [Eq. (6)] does not capture the emergence of the discontinuous transitions for $l > \sqrt{2}$, i.e., for large voltages $V > E_c L/4$. The stability analysis of the domain solution (4) that we perform below to describe the large-voltage regime is based on the Lyapunov functional (LF) approach to the ZRS problem [11]. The advantage of the LF method is that it is capable of discriminating the stable (global minimum of the LF) and metastable (local minimum) states that can be distant in phase space. The LF $\Phi\{E(x)\} = -G + K$ is given by the difference of the gain $G = -\int dx \int_0^{E(x)} dE' E' \sigma(E')$ and the DW contribution $K = (D/2)\int dx E(x)\hat{C}E(x)$, where the capacitance operator $\hat{C} = (\epsilon/2\pi)\partial_x \mathcal{H}$. For the model (1), we have

$$\Phi = -\int \frac{dx}{L}\sin^2\theta(x) + \lambda \int \frac{dx dx'}{2\pi L}\left[\frac{\theta(x) - \theta(x')}{x - x'}\right]^2, \quad (11)$$

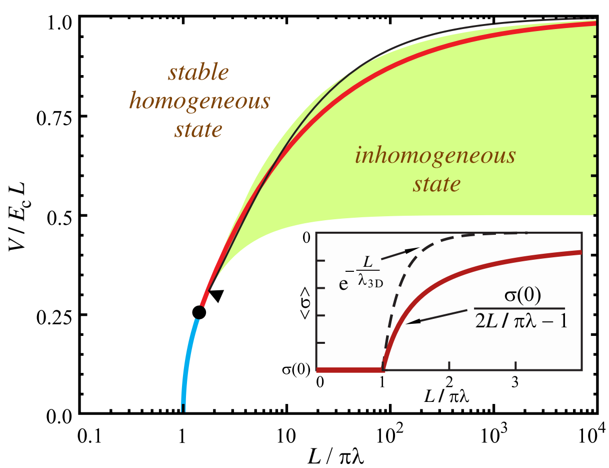


FIG. 3 (color online). Phase diagram of the voltage-biased stripe in the $V$-$L$ plane ($V$ and $L$ measured in units of $E_c L$ and $\pi\lambda$, respectively). The phase boundary (solid line), induced by the longitudinal instability, separates the homogeneous (above) and domain (below) states. In the unbiased stripe, there is a second-order phase transition at $L/\pi\lambda = 1$. The continuous transition line terminates with increasing $V$ and $L$ at the tricritical point (filled circle) $V = E_c L/4$, $L/\pi\lambda = \sqrt{2}$. At larger $V$ and $L$, the transition is first order. The shaded area is the region of hysteresis. The thin line, with the end point marked by the triangle, denotes the linear stability threshold for the homogeneous state against transverse fluctuations. Inset: the effective linear-response conductivity $\langle\sigma\rangle$ as a function of $L$. The dashed line shows $\langle\sigma\rangle$ for a 3D medium [8,26].

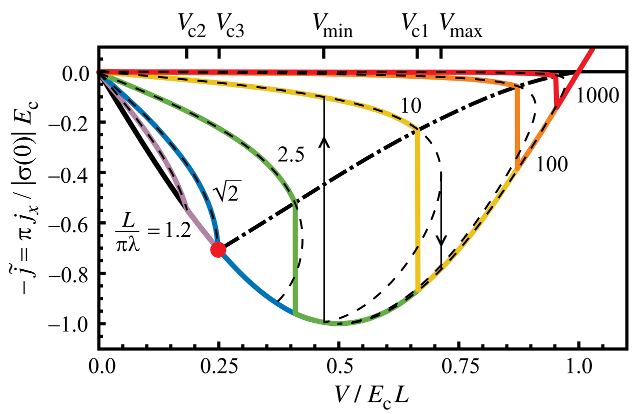


FIG. 4 (color online). Current-voltage characteristic (thick lines) of the stripe for different $L/\pi\lambda$ values. For $L/\pi\lambda < 1$ (homogeneous state), the dependence of the dissipative current $j_x(V)$ is given by the lowest curve $\tilde{j} = \sin(\pi V/E_c L)$. For $1 < L/\pi\lambda < \sqrt{2}$, the homogeneous state breaks up into domains for $V < V_{c2}$, in a continuous fashion, and the $j_x$-$V$ curve has a kink, as shown for $L/\pi\lambda = 1.2$. For $L/\pi\lambda > \sqrt{2}$, the $j_x$-$V$ curves for the domain state (dashed lines) are double valued and the transition becomes discontinuous, as demonstrated by the jumps of $j_x(V)$ at $V = V_{c1}$ (the critical voltage is marked for $L/\pi\lambda = 10$) in the curves for $L/\pi\lambda = 2.5$, 10, 100, 1000. The discontinuous transition line (dash-dotted line) terminates at the tricritical point (filled circle) at $V = V_{c3}$. The arrows on the thin vertical lines denote hysteresis (shown for $L/\pi\lambda = 10$) in the interval $V_{\min} < V < V_{\max}$.

which gives $\Phi_{\rm hom} = -\sin^2\theta_{\rm hom}$ in the uniform state and

$$\Phi_{\rm dom} = -\left(1+\sqrt{1-\tilde{j}^2}\right)/2 + l^{-1} - l^{-1}\ln\sqrt{\tilde{j}^2 + l^{-2}} \qquad (12)$$

in the domain state (4).

*First-order transitions.*—Comparison of $\Phi_{\rm hom}$ and $\Phi_{\rm dom}$ leads to the phase boundary (thick line) in Fig. 3 and the CVCs (thick lines) for different $l$ in Fig. 4. For $l < 1$, the homogeneous state is stable ($\Phi_{\rm hom} < \Phi_{\rm dom}$) for arbitrary $V$. For a given $l$ in the interval $1 < l < \sqrt{2}$, there is a continuous voltage-driven transition ($\Phi_{\rm hom} = \Phi_{\rm dom}$) between the homogeneous and domain states at $V = V_{c2} \equiv (E_c L/\pi)\arccos l^{-1}$. For $l > \sqrt{2}$, there emerges the interval $V_{\rm min} < V < V_{\rm max}$ (whose end points are shown in Fig. 4 for $l = 10$) in which the function $\tilde{j}(V)$ for the domain state is double valued (dashed lines in Fig. 4). Note that the expression for $V_{\rm min}$ coincides with that for $V_{c2}$ so that $V_{\rm min}$ saturates as $l$ is increased at $E_c L/2$. On the lower branch (with $dV/dj_x > 0$), $\Phi_{\rm dom}$ is greater than its value on the upper branch (and the lower branch is unstable against linear fluctuations [31], see also Ref. [33]). For the upper branch, the phase boundary equation $\Phi_{\rm hom} = \Phi_{\rm dom}$ (whose solution is shown in Fig. 4 as a dash-dotted line) yields, for $l > \sqrt{2}$, the first-order transition at $V = V_{c1}$, where $V_{c1}$ tends to $E_c L$ in the "bulk" limit $l \to \infty$ as $V_{c1}/E_c L \simeq 1 - (1/\pi)(2\ln l/l)^{1/2}$ [34]. The discontinuity in $\tilde{j}$ [which vanishes as $(2\ln l/l)^{1/2}$ for $l \gg 1$], between the upper-branch domain state and the homogeneous state, is illustrated by the vertical thick lines in Fig. 4. The "tricritical" point, separating the first- and second-order transitions, at $l = \sqrt{2}$ and $V = V_{c3} \equiv E_c L/4$ is marked by the filled circles in Figs. 3 and 4 [35].

In the above, we assumed that the system resides in the stable state. The domain state for $V_{c1} < V < V_{\rm max}$ and the homogeneous state for $V_{\rm min} < V < V_{c1}$ are metastable; i.e., they can be probed if the voltage sweep rate is larger than their characteristic decay rates. In this (nonadiabatic) limit, the system exhibits hysteresis [36], as marked in Fig. 4 by the arrows on the thin vertical lines for the case of $l = 10$. The hysteresis range $V_{\rm min} < V < V_{\rm max}$ for arbitrary $l > \sqrt{2}$ is shown as a shaded area in Fig. 3.

*Transverse instability.*—Before concluding, we briefly comment on the stability of the above picture against transverse fluctuations. Starting from Eq. (5), these can be shown [31] to be irrelevant on the stability boundary (6) in Fig. 3 for a sufficiently narrow stripe with $l < l_{c\perp} \simeq 1.76$ (or equivalently, $V < V_{c\perp} \simeq 0.31 E_c L$). The threshold is marked in Fig. 3 by the triangle. The range of $l < l_{c\perp}$ includes the zero-bias critical point at $l = 1$ and the tricritical point at $l = \sqrt{2}$. For $l > l_{c\perp}$, the linear transverse stability is maintained above the thin line in Fig. 3, which runs well above the longitudinal stability threshold $V_{\rm min}$ for the homogeneous state (6) and very close to the discontinuous transition line $V_{c1}$ obtained for frozen transverse fluctuations. At $l = l_{c+} \simeq 7$, the two lines intersect so that for $l > l_{c+}$ the homogeneous state is unstable above $V_{c1}$. In the narrow region between the lines for $l > l_{c+}$, the global minimum of the LF should thus be given by a 2D domain state with broken translational invariance along the stripe. The nature of this state as well as the position of the boundary $V_{c1}^*$ for the global stability of the domain state (4) [37] requires additional study.

*Summary.*—We have studied transport in the voltage-biased stripe with a negative absolute conductivity and obtained the phase diagram that shows phase transitions between the domain and homogeneous states. The transitions are second order for small and first order for large voltages (Fig. 3). We have calculated the CVC of the domain state (Fig. 4) and found the negative dissipative conductance. Our predictions can be verified by measuring the CVC in sufficiently small samples in the vicinity of the ZRS transition.

We thank S. Dorozhkin, Y. Galperin, A. Kamenev, P. Ostrovsky, I. Protopopov, J. Smet, R. Suris, and M. Zudov for interesting discussions. The work was supported by the DFG-RFBR (I. A. D. and A. D. M.) and by the University of Iowa (M. K.).

[1] R. G. Mani, J. H. Smet, K. von Klitzing, V. Narayanamurti, W. B. Johnson, and V. Umansky, Nature (London) **420**, 646 (2002).
[2] M. A. Zudov, R. R. Du, L. N. Pfeiffer, and K. W. West, Phys. Rev. Lett. **90**, 046807 (2003).
[3] C. L. Yang, M. A. Zudov, T. A. Knuuttila, R. R. Du, L. N. Pfeiffer, and K. W. West, Phys. Rev. Lett. **91**, 096803 (2003).
[4] D. Konstantinov and K. Kono, Phys. Rev. Lett. **105**, 226801 (2010).
[5] I. A. Dmitriev, A. D. Mirlin, D. G. Polyakov, and M. A. Zudov, Rev. Mod. Phys. **84**, 1709 (2012).
[6] A. V. Andreev, I. L. Aleiner, and A. J. Millis, Phys. Rev. Lett. **91**, 056803 (2003).
[7] M. G. Vavilov and I. L. Aleiner, Phys. Rev. B **69**, 035303 (2004).
[8] A. F. Volkov and V. V. Pavlovskii, Phys. Rev. B **69**, 125305 (2004).
[9] J. Alicea, L. Balents, M. P. A. Fisher, A. Paramekanti, and L. Radzihovsky, Phys. Rev. B **71**, 235322 (2005).
[10] I. A. Dmitriev, M. G. Vavilov, I. L. Aleiner, A. D. Mirlin, and D. G. Polyakov, Phys. Rev. B **71**, 115316 (2005).
[11] A. Auerbach, I. Finkler, B. I. Halperin, and A. Yacoby, Phys. Rev. Lett. **94**, 196801 (2005); I. Finkler, B. I. Halperin, A. Auerbach, and Y. Yacoby, J. Stat. Phys. **125**, 1093 (2006).
[12] I. G. Finkler and B. I. Halperin, Phys. Rev. B **79**, 085315 (2009).
[13] R. L. Willett, L. N. Pfeiffer, and K. W. West, Phys. Rev. Lett. **93**, 026804 (2004).
[14] M. A. Zudov, R. R. Du, L. N. Pfeiffer, and K. W. West, Phys. Rev. Lett. **96**, 236804 (2006).
[15] W. Zhang, M. A. Zudov, L. N. Pfeiffer, and K. W. West, Phys. Rev. Lett. **98**, 106804 (2007); A. T. Hatke, H.-S.

Chiang, M. A. Zudov, L. N. Pfeiffer, and K. W. West, Phys. Rev. B **77**, 201304(R) (2008).

[16] S. Wiedmann, G. M. Gusev, O. E. Raichev, A. K. Bakarov, and J. C. Portal, Phys. Rev. Lett. **105**, 026804 (2010).

[17] A. A. Bykov, JETP Lett. **91**, 361 (2010).

[18] S. I. Dorozhkin, L. Pfeiffer, K. West, K. von Klitzing, and J. H. Smet, Nat. Phys. **7**, 336 (2011).

[19] D. Konstantinov, A. Chepelianskii, and K. Kono, J. Phys. Soc. Jpn. **81**, 093601 (2012).

[20] A. T. Hatke, M. A. Zudov, J. D. Watson, and M. J. Manfra, Phys. Rev. B **85**, 121306(R) (2012).

[21] A. F. Volkov and Sh. M. Kogan, Sov. Phys. Usp. **11**, 881 (1969).

[22] V. L. Bonch-Bruevich, I. P. Zvyagin, and A. G. Mironov, *Domain Electrical Instabilities in Semiconductors* (Consultants Bureau, New York, 1975).

[23] J. B. Gunn, Solid State Commun. **1**, 88 (1963).

[24] P. F. Liao, A. M. Glass, and L. M. Humphrey, Phys. Rev. B **22**, 2276 (1980); S. A. Basun, A. A. Kaplyanskii, and S. P. Feofilov, JETP Lett. **37**, 586 (1983).

[25] S. A. Basun, A. A. Kaplyanskii, S. P. Feofilov, and A. S. Furman, JETP Lett. **39**, 189 (1984); S. A. Basun, A. A. Kaplyanskii, and S. P. Feofilov, Sov. Phys. JETP **60**, 1182 (1984).

[26] M. I. Dyakonov, JETP Lett. **39**, 185 (1984); M. I. Dyakonov and A. S. Furman, Sov. Phys. JETP **60**, 1191 (1984).

[27] For $P - P_c \ll P_c$, the field $E_c$ scales as $|\sigma(0)|^{1/2}$ [5].

[28] This condition means that the nonequilibrium screening length $\lambda$ [Eq. (3)], which diverges at $\sigma(0) \rightarrow 0$, is greater than the cyclotron radius and the inelastic scattering length [5].

[29] I. A. Dmitriev, S. I. Dorozhkin, and A. D. Mirlin, Phys. Rev. B **80**, 125418 (2009).

[30] This model function allows for an exact analytical solution to Eq. (1), whereas the physics the solution reveals is insensitive to the exact shape of the single-parameter function $\sigma(E)$.

[31] I. A. Dmitriev, M. Khodas, A. D. Mirlin, and D. G. Polyakov (unpublished).

[32] S. I. Dorozhkin, I. A. Dmitriev, and A. D. Mirlin, Phys. Rev. B **84**, 125448 (2011).

[33] F. G. Bass, V. S. Bochkov, and Yu. G. Gurevich, Sov. Phys. JETP **31**, 972 (1970).

[34] It is worth emphasizing that our consideration was performed in the mean-field framework. The impact of fluctuations on this problem remains to be studied. In particular, one can apply the methods of Ref. [9] where it was found (in the limit $V \rightarrow 0$ and $L \rightarrow \infty$) that fluctuations may force the ZRS transition to be first order. Remarkably, we obtain the first-order transition driven by finite voltage already on the mean-field level.

[35] There are formal similarities between the ZRS transition and the overheating instability leading to the formation of electron temperature domains in a current-carrying slab [33]. In both cases, the transitions are second order in narrow and first order in wide samples.

[36] The obtained hysteresis bears close similarity to the nonequilibrium first-order phase transition proposed in Ref. [26] to describe the experiment [24,25] on illuminated ruby crystals. The key differences between our problem and that in Ref. [26] are the importance of transverse fluctuations, which are absent in the model of Ref. [26], and the nonlocal character of 2D electrostatics. We also found a richer behavior of the system by studying the case of smaller system sizes $L/\pi\lambda \sim 1$, where the tricritical point and the continuous phase transitions emerge.

[37] We were able to check numerically that the linear stability threshold of the domain state (4) remains above $V_{c1}$; i.e., the state (4) is linearly stable in the whole region $V < V_{c1}$, at least for $l < 40$.